Real-Space Spectral Approach to Orbital Magnetization

Kevin J. U. Vidarte,[1]
Henrique P. Veiga,[2,3]
João M. Viana Parente Lopes,[2]
Ramon Cardias,[4]
Aires Ferreira,[3]
Tarik P. Cysne,[5]
Tatiana G. Rappoport[1,4,6]
[1]*International Iberian Nanotechnology Laboratory (INL), Av. Mestre José Veiga, 4715-330 Braga, Portugal.*
[2]*Centro de Física das Universidades do Minho e Porto Departamento de Física e Astronomia, Faculdade de Ciências, Universidade do Porto, 4169-007 Porto, Portugal*
[3]*School of Physics, Engineering and Technology and York Centre for Quantum Technologies, University of York, York YO10 5DD, United Kingdom*
[4]*Centro Brasileiro de Pesquisas Físicas (CBPF), Rua Dr Xavier Sigaud 150, Urca, 22290-180, Rio de Janeiro-RJ, Brazil*
[5]*Instituto de Física, Universidade Federal Fluminense, 24210-346 Niterói RJ, Brazil*
[6]*Physics Center of Minho and Porto Universities (CF-UM-UP),Campus of Gualtar, 4710-057, Braga, Portugal*
kevin.urcia@inl.int

We present a real-space spectral method for computing the orbital magnetization of crystals. Starting from the commutator form of the orbital magnetization operator, we formulate an energy resolved spectral function that is amenable to exact Chebyshev polynomial expansions and yields the total magnetization upon integration up to the Fermi level. This avoids the need for computing eigenstates and ground-state projects, providing an efficient numerical framework that is applicable to very large systems even in the presence of disorder and temperature. Our approach is bench marked on the Haldane model, finding results that are in excellent agreement with the modern k-space formulation of orbital magnetization. Leveraging this technique, we extend our study to systems with uncorrelated disorder and point defects, and further show that the bulk Chern number can be directly obtained from the magnetization spectral density. These results open a promising route to investigate orbital responses and topological transitions in real-space models of quantum materials with realistic complexity.

References

[1] T. P. Cysne, L. M. Canonico, M. Costa, R. B. Muniz, and T. G. Rappoport, Orbitronics in two-dimensional mate rials, npj Spintronics 3, 39 (2025).
[2] R. Bianco and R. Resta, Orbital magnetization as a local property, Phys. Rev. Lett. 110, 087202 (2013).
[3] R. Bianco and R. Resta, Mapping topological order in coordinate space, Phys. Rev. B 84, 241106 (2011).
[4] D. Ceresoli, T. Thonhauser, D. Vanderbilt, and R. Resta, Orbital magnetization in crystalline solids: Multi-band insulators, chern insulators, and metals, Phys. Rev. B 74, 024408 (2006).
[5] T. Thonhauser, D. Ceresoli, D. Vanderbilt, and R. Resta, Orbital magnetization in periodic insulators, Phys. Rev. Lett. 95, 137205 (2005).
[6] A. Marrazzo and R. Resta, Irrelevance of the boundary on the magnetization of metals, Phys. Rev. Lett. 116, 137201 (2016).
[7] M. G. Lopez, D. Vanderbilt, T. Thonhauser, and I. Souza, Wannier-based calculation of the orbital magnetization in crystals, Phys. Rev. B 85, 014435 (2012)
[8] D. Seleznev and D. Vanderbilt, Towards a theory of sur face orbital magnetization, Phys. Rev. B 107, 115102 (2023).

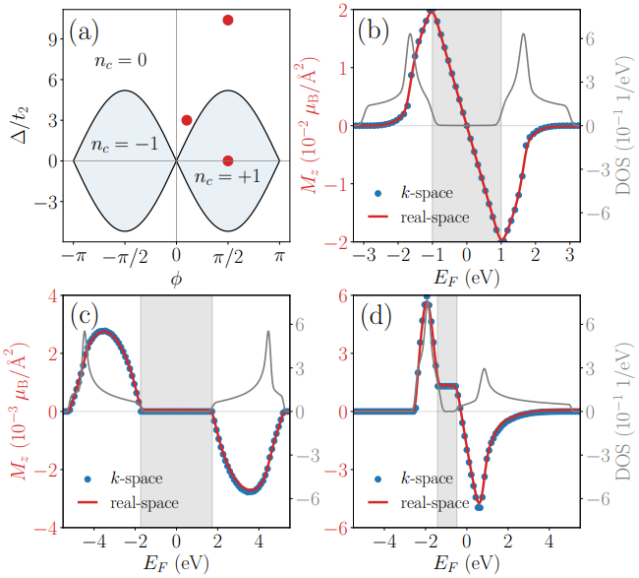

Figure 1: (a) Topological phase diagram showing the Chern number of the bottom band as a function of ϕ and Δ/t2. Red points (ϕ, Δ/t2) = (0.5π, 0), (0.5π, 6 √ 3) and (0.1π, 3) indicate the parameters for panels (b), (c) and (d), respectively. (b-d) Orbital magnetization (red lines) in real-space formulation and density of states (grey lines) as functions of the energy. The blue dots show the results of the reciprocal-space formulation. In our Chebyshev approach, we simulate a large rectangular domain with 106 sites. Other parameters: M = 200 and R = 800.

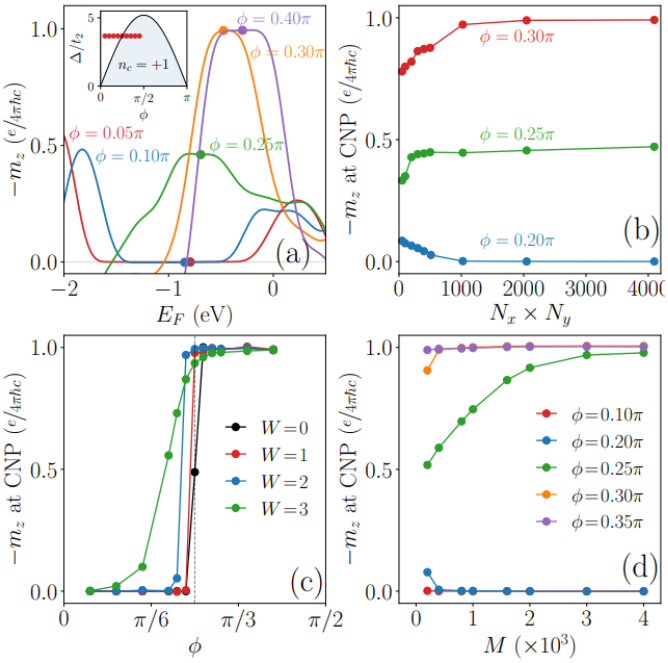

Figure 2: Chern number from the orbital magnetization: Panel (a) plots $-m_z$, calculated within the band gap for pristine systems at Δ/t2 = 3√ 3 sin(π/4) and ϕ = 0.05π, 0.10π, 0.25π, 0.30π and 0.40π. The coloured dots on each curve denote the respective CNP values. The inset represents the Chern number of the valence band of the Haldane model. The red points in this phase diagram are relevant for the subsequent discussion and figures. Panel (b) plots −mz at the CNP as a function of the sample sizes for pristine systems with ϕ = 0.20π, 0.25π and 0.30π. The panel (c) plots −mz at the CNP as functions of ϕ with D ≈ 4 × 106 , M = 4000 and R = 2000. The panel (d) plots −mz at the CNP as functions of M for W = 1 with D ≈ 4 × 106 and R = 2000.